Theoret. Chim. Acta (Berl.) 57, 145–161 (1980)

THEORETICA CHIMICA ACTA

Approximate Franck–Condon Factors from Piecewise Langer-Transformed Vibrational Wave Functions

Heinz Krüger

Fachbereich Physik der Universität Kaiserlautern, Postfach 3049, D-6750 Kaiserslautern, Federal Republic of Germany

An accurate normalization prescription is derived and tested for approximate bound vibrational wavefunctions due to W. H. Miller [1]. These bound state- and single turning point uniform Langer transformed continuum functions then are used to approach all types of Franck–Condon transition elements via partially uniform mapping techniques in a three dimensional space of integration variables. The classical Franck–Condon principle, Mulliken's difference potential, various reflection approximations and many other of the more recent approaches are shown to be naturally included in our method. The excellent accuracy of the final results is demonstrated by comparing with exact Franck–Condon matrix elements of Stückelberg's bound–continuum model.

Key words: Continuum-continuum, bound–continuum and bound–bound Franck–Condon factors – Semiclassical matrix elements – Excimer lasers.

1. Introduction

Approximate vibrational wave functions to a two-turning point anharmonic well have been obtained by W. H. Miller [1] by matching two Airy-uniform wave function pieces [2] at some convenient midphase point. Miller aimed at deriving some improved quantum condition, which especially for lowlying vibrational states should be of better accuracy as the conventional WKB condition. In Ref. [1] however, Miller did not derive the normalization factors to his wave functions, even though he implicitly made use of them when calculating Franck–Condon factors in Sect. III of his paper.

0040-5744/80/0057/0145/$03.40

Since we are concerned here with (partially) uniform evaluations of Franck–Condon (FC) factors, we need those normalization constants, or, at least some very accurate approximations to them. This fixes the plan of this paper:

In Sect. 2 we derive an accurate expression for the normalization constant of Miller's wavefunction by exploiting a Wronski determinantal relationship. This and a simplified version of this expression then is used to present an accuracy test of Miller's functions in case of the harmonic oscillator.

In Sect. 3, various FC integrals (bound–continuum, bound–bound, etc.) are evaluated in some semiclassical approximation by making use of stationary phase mapping techniques in a three dimensional space of integration variables. In the sense of stationary phase integration, the main contributions to the FC integrals are seen to come from small regions (points) which satisfy in some subspace the FC principle or the difference potential concept introduced by Mulliken [3].

In Sect. 4 several reflection approximations and other limiting forms are derived from the general treatment in Sect. 3.

Finally, in Sect. 5, the accuracy of our semiclassical approximation is checked by a numerical comparison with the exact FC integrals of Stückelberg's bound–continuum model [4].

2. Normalization of Piecewise Airy-Uniform Bound State Functions

As mentioned above, W. H. Miller [1] has composed approximate vibrational wave functions for an anharmonic potential $V(x)$ from two pieces, each of which is an Airy-uniform Langer function at either turning point x_1, x_2, $x_1 < x_2$. See Fig. 1 for a schematic description of the continuous derivative matching of the two wave function pieces at the midphase point x_0. Miller's results can briefly be summarized as follows. The wave function of a bound state with the nodenumber n can be written in the form

$$\varphi_n(x) = a(x)\mathcal{A}i(z(x)), \tag{1}$$

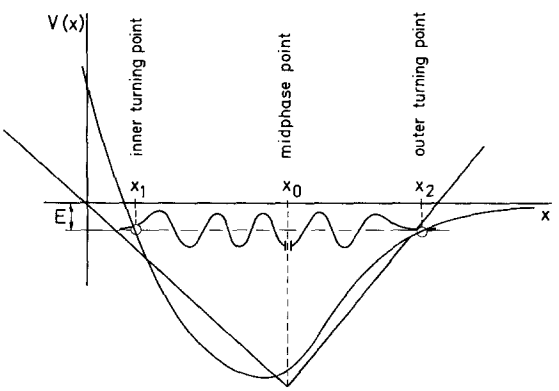

Fig. 1. Matching of the two Airy-uniform Langer functions

$$a(x) = C_n(x)|z'(x)|^{-1/2} \tag{2}$$

$$C_n(x) = D_n \begin{cases} (-1)^n, & \text{for } -\infty \leq x \leq x_0 \\ 1, & \text{for } x_0 \leq x \leq +\infty, \end{cases} \tag{3}$$

where $z(x)$ is the continuous union of solutions of

$$z'^2 z = \frac{2m}{\hbar^2}[V(x) - E_n] = u(x), \tag{4}$$

which for $x \leq x_0$ vanishes at the inner turning point x_1

$$z(x_1) = 0, \quad \text{for } x \leq x_0 \tag{5}$$

and for $x_0 \leq x$ vanishes at the outer turning point x_2

$$z(x_2) = 0, \quad \text{for } x_0 \leq x. \tag{6}$$

The midphase point x_0 is determined by

$$\int_{x_0}^{x_2} dx\, k(x) = \int_{x_1}^{x_0} dx\, k(x) = \Phi/2 \tag{7}$$

$$\Phi = \int_{x_1}^{x_2} dx\, k(x) \equiv \Phi(E_n), \qquad \hbar k(x) = \sqrt{2m[E_n - V(x)]}, \tag{8}$$

which depends on the binding energies E_n. The values E_n are fixed by the modified WKB condition

$$\Phi(E_n) = \pi(N_n + 1/2), \tag{9}$$

where the *noninteger* numbers N_n are given by

$$N_n = \begin{cases} \frac{4}{3\pi}[A_{(n+1)/2}]^{3/2} - \frac{1}{2}, & \text{for } n = 1, 3, 5, \ldots \text{ (odd)} \\ \frac{4}{3\pi}[B_{(n+2)/2}]^{3/2} - \frac{1}{2}, & \text{for } n = 0, 2, 4, \ldots \text{ (even).} \end{cases} \tag{10}$$

The real, positive number A_s is the sth zero of

$$\mathcal{A}i\,(-A_s) = 0, \qquad s = \frac{n+1}{2} \tag{11}$$

and B_t is the tth real, positive zero of

$$\mathcal{A}i\,(-B_t) - 4B_t\,\mathcal{A}i'(-B_t) = 0, \qquad t = \frac{n+2}{2}. \tag{12}$$

As seen by inspection of Table 1 in [1], the numbers N_n deviate from the corresponding integers in the WKB condition less than 6%. Clearly, this means that e.g. for the harmonic oscillator, Miller's modified quantum condition (9) is less accurate than the WKB condition, which in this case is exact. For the quartic

oscillator however, condition (9) gives better energy values than the usual WKB condition.

If one wishes to use the bound state functions (1) for calculating FC integrals, it is necessary to determine the still unknown normalization constants D_n in Eq. (3). The evaluation of the normalization integral

$$I_n = \int_{-\infty}^{+\infty} dx\, \varphi_n^2(x) \tag{13}$$

can be performed with the help of the Wronski relation applied in [5]. Neglecting, as in [5], Schwarzian derivative corrections, we note from Eqs. (1)–(4) that $\varphi(x) \equiv \varphi(E, x)$ for $E \neq E_n$ satisfies the differential equation

$$\left\{\frac{d^2}{dx^2} + \frac{2m}{\hbar^2}[E - V(x)]\right\}\varphi(E, x) = 0, \tag{14}$$

which as in [5] leads to

$$\frac{2m}{\hbar^2}\int_\alpha^\beta dx\, \varphi^2(E, x) = \left[\frac{\partial\varphi}{\partial E}\frac{\partial\varphi}{\partial x} - \varphi\frac{\partial^2\varphi}{\partial x\,\partial E}\right]_{x=\alpha}^{x=\beta} \equiv W_x(\varphi_E, \varphi)\Big|_{x=\alpha}^{x=\beta}, \tag{15}$$

valid for any finite integration interval $\langle\alpha, \beta\rangle$ *not containing the midphase point* x_0. Since because of $E \neq E_n$, the first derivative of $\varphi(E, x)$ with respect to x, $\partial\varphi/\partial x$, *is discontinuous*, but $\varphi(E, x)$ still vanishes at the boundaries $x = \pm\infty$, we find, upon applying (15) separately to the left and to the right of the midphase point x_0,

$$\begin{aligned}\frac{2m}{\hbar^2}\int_{-\infty}^{+\infty} dx\, \varphi^2(E, x) &= \lim_{\varepsilon\to 0_+}\{W_x(\varphi_E, \varphi)|_{x=x_0-\varepsilon} - W_x(\varphi_E, \varphi)|_{x=x_0+\varepsilon}\} \\ &\equiv \frac{2m}{\hbar^2} I(E).\end{aligned} \tag{16}$$

After having evaluated this limit, $I(E)$ then finally yields the desired integral (13) for $E = E_n$,

$$I_n = I(E_n). \tag{17}$$

We do not intend to present the details of this straightforward but quite tedious calculation. We rather give the result

$$I_n = D_n^2 \frac{\hbar^2}{2m\pi}\frac{d\Phi(E_n)}{dE_n}\mu_n, \tag{18}$$

where

$$\mu_n = \pi\begin{cases}[\mathrm{Ai}'(-A_{(n+1)/2})]^2 (A_{(n+1)/2})^{-1/2}, & \text{for } n = 1, 3, 5, \ldots \\ [\mathrm{Ai}'(-B_{(n+2)/2})]^2 (16B_{(n+2)/2} + 5)(B_{(n+2)/2})^{-1/2}, & \text{for } n = 0, 2, 4, \ldots .\end{cases} \tag{19}$$

Hence, if the $\varphi_n(x)$ in (1) shall be normalized according to

$$\int_{-\infty}^{+\infty} dx\, \varphi_n^2(x) = 1, \tag{20}$$

Table 1. Quantum constants N_n, Eq. (10) and the coefficients $\mu_n^{-1/2}$, Eq. (21) for various nodenumbers n

n	N_n	$\mu_n^{-1/2}$
0	0.060331748	0.94334586
1	1.0173492	0.99493009
2	2.0115048	0.99761516
3	3.0078995	0.99890841
4	4.0063030	0.99928937
5	5.0050789	0.99954491
10	10.002685	0.99987177
15	15.001814	0.99994160
20	20.001373	0.99996644
30	30.000923	0.99998482
40	40.000695	0.99998466
50	50.000557	0.99998878
70	70.000399	0.99999548
100	100.00028	0.99999857

the constants D_n in Eq. (3) are to be fixed according to

$$D_n = \left[\frac{2m\pi}{\hbar^2\Phi'(E_n)}\right]^{1/2} \mu_n^{-1/2}. \tag{21}$$

In Table 1 the quantum constants N_n (Eqs. (9), (10)) and the values $\mu_n^{-1/2}$ needed in (21) are listed for several nodenumbers n. We note, that for nodenumbers $n \gtrsim 1$ one may safely replace Eq. (21) by the simpler expression

$$D_n \simeq \left[\frac{2m\pi}{\hbar^2\Phi'(E_n)}\right]^{1/2}, \tag{22}$$

the accuracy of which reflects the fact that state densities and hence the normalization constants of bound state functions are adiabatic invariants. This suggests a more convenient version for calculating the normalized bound state functions (1). Replace Eq. (10) just by

$$N_n \simeq n \tag{23}$$

and replace Eq. (21) by Eq. (22). The search of the midphase value x_0 in general however has to be done numerically, if it is not anyway fixed by the symmetry of the potential well. Let us distinguish such a bound state function obtained via this simplified procedure from an accurate one, $\varphi_n(x)$, by attaching a subscript "s". In Table 2, several values of $\varphi_n(x)$ and $\varphi_{sn}(x)$ are compared with the corresponding exact eigen functions

$$\psi_n(x) = H_n(x)\, e^{-x^2/2} 2^{-n/2} (n!)^{-1/2} \pi^{-1/4} \tag{24}$$

of a harmonic oscillator with the potential $(2m/\hbar^2)V(x) = x^2$. We note that φ and φ_s are of roughly the same accuracy. In spite of the simpler numerical procedure φ_s should be used preferentially. We also note that close to a zero of the exact wave function ψ, the relative errors of φ and φ_s clearly may increase (as seen e.g. for $n = 60$, $x = 0.7$ or 5.2). But this would not affect the accuracy of integrals

Table 2. Comparison of Miller's bound state functions $\varphi_n(x)$, $\varphi_{sn}(x)$ with the exact eigen functions $\psi_n(x)$ of a harmonic oscillator, Eq. (24). The numbers in parentheses denote the power of 10 by which the value in front must be multiplied

n	x	$\psi_n(x)$	$\varphi_{sn}(x)$	$\left\|1-\frac{\varphi_s}{\psi}\right\|\cdot 10^2$	$\varphi_n(x)$	$\left\|1-\frac{\varphi}{\psi}\right\|\cdot 10^2$
	0.1	0.7474	0.7630	2.08	0.7109	4.87
	0.4	0.6934	0.6936	0.03	0.6634	4.32
0	1.6	0.2088	0.2035	2.6	0.2065	1.14
	2.8	1.49(−2)	1.44(−2)	3.1	1.51(−2)	1.39
	5.0	2.7992(−6)	2.7043(−6)	3.4	2.9276(−6)	4.59
	0.0	−0.5311	−0.5324	0.24	−0.5306	0.10
	0.2	−0.4790	−0.4764	0.53	−0.4788	4.(−2)
	0.4	−0.3334	−0.3284	1.49	−0.3340	0.19
2	0.8	0.1080	0.1137	5.29	0.1058	2.05
	1.6	0.6084	0.6086	5.(−2)	0.6071	0.21
	3.2	6.18(−2)	6.15(−2)	0.53	6.21(−2)	0.35
	0.0	0.315291	0.315303	3.8(−3)	0.315288	9.(−4)
	0.5	−0.315257	−0.315233	7.6(−3)	−0.315254	7.(−4)
20	2.0	0.323322	0.323317	1.6(−3)	0.323317	1.6(−3)
	5.0	−0.395581	−0.395567	3.4(−3)	−0.395579	5.(−4)
	6.0	0.496804	0.496795	1.9(−3)	0.496797	1.4(−3)
	8.0	1.2241(−3)	1.2235(−3)	5.1(−2)	1.2247(−3)	4.5(−2)
	0.0	0.2405692	0.2405703	4.(−4)	0.2405680	5.(−4)
	0.7	3.81400(−2)	3.79825(−2)	0.4	3.81489(−2)	2.3(−2)
	2.6	−0.2436397	−0.2436462	2.7(−3)	−0.2436460	1.(−4)
60	5.2	3.9088(−3)	4.001(−3)	2.36	3.8725(−3)	0.93
	8.3	0.2969036	0.2969042	2.(−4)	0.2969012	8.(−4)
	11.5	6.83364(−2)	6.83304(−2)	9.(−3)	6.83405(−2)	6.1(−3)
	14.0	6.195(−8)	6.194(−8)	1.5(−2)	6.196(−8)	1.5(−2)

performed with the functions φ_s or φ. Thus, the simplified version φ_s of Miller's bound state functions is ideally suited for approaching FC integrals.

3. Approximation Calculation of FC Integrals

Recalling Eq. (23) of Ref. [5] and Eq. (1), we note that all types of FC integrals (continuum–continuum, bound–continuum and bound–bound) can be approximated within percent accuracy by

$$I = \int_{-\infty}^{+\infty} dx\, \rho(x)\, \mathcal{A}i\,(z_1(x))\, \mathcal{A}i\,(z_2(x)). \tag{25}$$

In Eq. (25) the function $\rho(x)$ may contain a dimensionless transition moment (e.g. an electronic transition moment) and other prefactors which occur in Eqs. (1), (2), (3) or in Eq. (23) of [5]. Important for the following steps is only one property of $\rho(x)$ which we take for granted, namely, that ρ is slowly varying compared to $\mathcal{A}i\,(z_1)$ or $\mathcal{A}i\,(z_2)$. That this assumption is very well satisfied for molecular bound-

or continuum functions is obvious, because in that case the typical variation range of $\mathcal{A}i(z_1)$ or $\mathcal{A}i(z_2)$ is the de Broglie wavelength of the molecular relative motion.

With the integral representation for the Airy function [6]

$$\mathcal{A}i(z)=\frac{1}{2\pi}\int_{-\infty}^{+\infty} dt \exp\left[i\left(\frac{t^3}{3}+zt\right)\right] \tag{26}$$

we can write (25) in the form

$$I=\frac{1}{4\pi^2}\int_{-\infty}^{+\infty} dx_1 \int_{-\infty}^{+\infty} dx_2 \int_{-\infty}^{+\infty} dx_3\, \rho(x_3) \exp\left[i\Phi(x_1, x_2, x_3)\right], \tag{27}$$

where the phase function Φ is given by

$$\Phi=\frac{x_1^3}{3}+\frac{x_2^3}{3}+x_1 z_1(x_3)+x_2 z_2(x_3). \tag{28}$$

Our aim now is, to relate the integral (27) to a simpler one which can be solved in closed form but has the same stationary point structure as (27). In this way [7–8] one obtains a uniform asymptotic approximation to (27) and hence to all types of FC factors. In order to do so, we first look for the stationary points of Φ. These are given by the (three) equations

$$\text{grad}\,\Phi=0, \tag{29}$$

which lead to the system

$$x_1^2+z_1(x_3)=0, \qquad x_2^2+z_2(x_3)=0, \qquad x_1 z_1'(x_3)+x_2 z_2'(x_3)=0. \tag{30}$$

Defining

$$u_i(x)=z_i(x)[z_i'(x)]^2, \qquad i=1, 2, \tag{31}$$

(30) can be decoupled to yield

$$u_1(x_3)=u_2(x_3) \tag{32}$$

for the $x_3=x$ co-ordinate (the integration variable in Eq. (25)) of the stationary points. In the sense of the stationary phase method Eq. (32) means, that the main contributions to the integral (25) come from those points which on the x-axis satisfy (32). If we recall Eq. (4) and Eq. (24) in [5], we note that in case of a transition from a potential (curve) $V_1(x)$ and energy E_1 to a potential $V_2(x)$ and energy E_2, Eq. (32) implies that *the main contribution to the* FC *integral comes from x-values which conserve the local kinetic energy*, viz.

$$V_1(x)-E_1=V_2(x)-E_2. \tag{33}$$

This is the famous FC principle [9], [3]. There are many ways of representing condition (33) graphically. Drawing the *difference potential* V_1-V_2, [10], is for our purpose awkward. We rather plot, as in Fig. 2, each side of Eq. (33) separately and look for crossings. Fig. 2 shows for a bound–continuum transition typically two (real) crossings x_a, x_b, $x_a<x_b$. Clearly, under special conditions on the

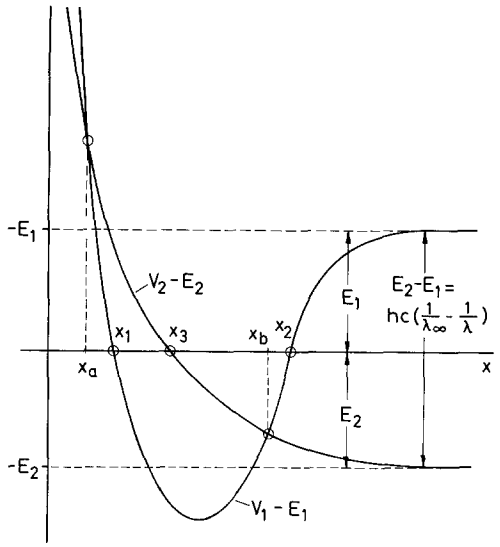

Fig. 2. Turning points x_1, x_2, x_3 and crossing points x_a, x_b for a bound–continuum transition

potential shape and energies, x_a and x_b may coincide and the two curves touch each other at $x_a = x_b$ with a common tangent. This situation is exceptional or atypical as it separates the large variety of two real crossings $x_a = x_b$ from the large variety of cases, where the two curves only come close together but without cutting each other over the real axis (complex conjugate crossings). We limit our considerations in the following to the typical situation of *two separate real crossings* $x_a \neq x_b$. Because of this limitation, we call the approach presented here *partially* uniform. A complete, uniform treatment which allows for passing from the two separate real crossings case through the tangency situation which even may occur at the turning points[1] to the case of the two complex conjugate crossings is defered to a forthcoming publication.

Assuming henceforth x_a and x_b well separated enough that in some small neighbourhood of x_a and x_b there is a smooth one-to-one mapping between the variables x_1, x_2, x_3 and y_1, y_2, y_3 which satisfies

$$\Phi(x_1, x_2, x_3) = \Psi(y_1, y_2, y_3), \tag{34}$$

where Φ is given by Eq. (28) and Ψ is

$$\Psi = \frac{y_1^3}{3} + \frac{y_2^3}{3} + y_1(ay_3 + b) + y_2(cy_3 + d); \qquad a, b, c, d = \text{const.}\,. \tag{35}$$

If one chooses [12]

$$\begin{aligned} &a = z_1'(x_s), \qquad b = -x_s z_1(x_s), \\ &c = z_2'(x_s), \qquad d = -x_s z_2(x_s), \qquad x_s = x_a \text{ or } x_b, \end{aligned} \tag{36}$$

[1] This leads to the unfolding family of the swallowtail [11].

where $x_s = x_a$ if x_3 tends to x_a and $x_s = x_b$ if x_3 tends to x_b, Eq. (34) is satisfied at the stationary points, as can easily be verified by use of Eqs. (30)–(32). The polynomial Ψ is *a versal unfolding of* Φ, [11] Chap. 8, locally at $x_3 = x_a$ or $x_3 = x_b$. We do not prove this statement, we simply assume it to be true [13]. As seen from Eq. (36) it should be stressed that the one-to-one mapping between x- and y variables which acts at $x_3 = x_a$ (subscript a) is different from the mapping at $x_3 = x_b$ (subscript b). The two mappings represent two local coordinate systems or charts with domains $\mathscr{D}_a$ and $\mathscr{D}_b$ into which the integral (27) can be decomposed and we find with Eq. (34)

$$4\pi^2 I = \int_{\mathscr{D}_a} d^3 y_a |J_a| \rho_a \, \mathrm{e}^{i\Psi_a} + \int_{\mathscr{D}_b} d^3 y_b |J_b| \rho_b \, \mathrm{e}^{i\Psi_b}, \tag{37}$$

where $|J_a|$ or $|J_b|$ is the absolute value of the Jacobian for the two mappings

$$J = \det\left(\frac{\partial x_i}{\partial y_k}\right), \qquad i, k = 1, 2, 3, \tag{38}$$

in either chart a or b. The *leading* asymptotic term of each of the two integrals in (37) can be obtained in a nonrigorous but simple way. One just puts the factors $|J|\rho$ at their stationary values $x_3 = x_a$ or $x_3 = x_b$ and replaces the remaining integrals by the generic or canonical integral, [7] Chap. 4 and the Appendix of [12],

$$\tilde{I} = (2\pi)^{-2} \int d^3 y \, \mathrm{e}^{i\Psi} = \int_{-\infty}^{+\infty} dy \, \mathscr{A}i\,(ay + b)\, \mathscr{A}i\,(cy + d) = |a^3 - c^3|^{-1/3} \, \mathscr{A}i\,(\eta)$$

$$\eta = (a^3 - c^3)(ad - bc)|a^3 - c^3|^{-4/3}. \tag{39}$$

We note the manifest symmetry of Eq. (39) upon the interchange $a, b \leftrightarrow c, d$. From page 16 in Ref. [14] we infer that the Hessian determinant of Ψ evaluated in y-variables, H_Ψ, the Hessian determinant of Φ evaluated in x-variables, H_Φ, and the Jacobian (38) satisfy

$$H_\Psi = J^2 H_\Phi \tag{40}$$

at the stationary points. With Eq. (40), the leading asymptotic approximation to Eq. (37) can be written

$$I \simeq \sum_{s=a,\,b} I_s, \tag{41}$$

where

$$I_s = \rho(x_s)\left(\frac{H_{\Psi_s}}{H_{\Phi_s}}\right)^{1/2} \tilde{I}_s, \tag{42}$$

and the subscript s indicates that all quantities in Eqs. (39) and (36) are to be evaluated at the stationary points with $x_3 = x_s = x_a$ or $x_s = x_b$. If only one or even more than two real crossings x_s occur, the sum in Eq. (41) will have just as many terms as there are real crossings. Calculating the Hessian determinants H_Ψ and H_Φ from Eqs. (35) and (28) and simplifying by making repeated use of Eqs. (30)–(32),

one finds for I_s in Eq. (42) after some lengthy but straightforward algebra

$$I_s = \rho(x_s) \frac{|z_1'(x_s) z_2'(x_s)|^{1/2} \zeta_s^{1/4} \mathcal{A}i\left(\frac{u_1(x_s)}{|u_1(x_s)|}\zeta_s\right)}{|u_1(x_s)|^{1/4}|u_1'(x_s) - u_2'(x_s)|^{1/2}}, \tag{43}$$

where

$$\zeta_s = |\varepsilon_1(x_s)|z_1(x_s)|^{3/2} - \varepsilon_2(x_s)|z_2(x_s)|^{3/2}|^{2/3}, \tag{44}$$

and

$$\varepsilon_i(x) = \frac{z_i'(x)}{|z_i'(x)|}, \qquad i = 1, 2 \tag{45}$$

$$u_1(x_s) = u_2(x_s). \tag{46}$$

Again we note the exchange symmetry of Eqs. (43)–(46), (41) and Eq. (25) in z_1 and z_2. For the following it is useful to express the signs of z_1' and z_2' in Eq. (45) in terms of the signs of u_1' and u_2'. To this end we calculate the derivative of $u(x)$ in Eq. (4) or Eq. (31) at the turning point $x = x_1$ where $z(x_1) = 0$ (see Fig. 2). We find $u'(x_1) = [z'(x_1)]^3$ and hence $z'(x)$ has the same sign as $u'(x)$ at x_1. Since however $z(x)$ is a Langer mapping function, $z'(x)$ can not vanish in the interval $-\infty \leq x < x_0$ (see Eqs. (4), (5) and Fig. 1) and hence keeps the sign of $u'(x_1)$ by continuity. At $x = x_0$ however the sign of $z'(x)$ must change and stay constant for $x_0 < x \leq +\infty$ as a consequence of Eq. (6). The result is simple. The sign of $z'(x)$ agrees with the sign of the slope of $u(x)$ or with the sign of the slope of the potential $V(x)$ at the corresponding turning point. Thus, the sign of $z'(x)$ coincides with the sign of the slope of the two straight lines in Fig. 1 onto which $V(x)$ is mapped in two pieces by Langer transforms.

We close this section by writing down the (partially) uniform approximation which we obtain from Eqs. (41) and (43) for the FC integral with the transition moment $\mu(x)$ (electronic moment, r-centroid etc.)

$$M(E_1, V_1 \leftrightarrow E_2, V_2) = \int_{-\infty}^{+\infty} dx\, \varphi_{E_1 V_1}(x) \mu(x) \varphi_{E_2 V_2}(x) \tag{47}$$

to a transition between the potential $V_1(x)$ and energy E_1 (bound or continuum) and the potential $V_2(x)$, energy E_1 where the functions

$$u_i(x) = \frac{2m}{\hbar^2}(V_i(x) - E_i), \qquad i = 1, 2 \tag{48}$$

give rise to *two* real well separated crossings x_a, x_b, $x_a \neq x_b$, Eqs. (32), (33)

$$u_1(x_s) = u_2(x_s), \qquad s = a, b \tag{49}$$

as shown in Fig. 2. From Eqs. (1)–(6) or Ref. [5] Eqs. (23)–(26) and Eqs. (41)–(46) we find

$$M(E_1, V_1 \leftrightarrow E_2, V_2) \simeq \sum_{s=a,b} \frac{C_{E_1 V_1}(x_s) C_{E_2 V_2}(x_s) \mu(x_s) \zeta_s^{1/4} \mathcal{A}i(\varepsilon_s \zeta_s)}{|u_1(x_s)|^{1/4}|u_1'(x_s) - u_2'(x_s)|^{1/2}}, \tag{50}$$

where according to Eqs. (3) and (22)

$$C_{EV}(x)=\left(\frac{2m\pi}{\hbar^2\Phi'(E_n)}\right)^{1/2}\begin{cases}(-1)^n, & \text{for } -\infty\le x<x_0\\ 1, & \text{for } x_0<x\le+\infty\end{cases} \tag{51}$$

for bound states

$$C_{EV}(x)=\left(\frac{2m}{\hbar^2}\right)^{1/2} \tag{52}$$

for continuum states and

$$\zeta_s=|\varepsilon_1(x_s)|z_1(x_s)|^{3/2}-\varepsilon_2(x_s)|z_2(x_s)|^{3/2}|^{2/3}, \tag{53}$$

with

$$\varepsilon_i(x)=\text{sign}\,(z_i'(x)),\qquad i=1,2 \tag{54}$$

$$\varepsilon_s=\text{sign}\,(u_1(x_s))=\text{sign}\,(u_2(x_s)). \tag{55}$$

It is evident that the mapping functions z_i in Eq. (53) can be expressed in terms of action integrals. For bound states we find from Eqs. (4)–(6)

$$\tfrac{2}{3}|z_1(x)|^{3/2}=\begin{cases}\left|\int_{x_1}^{x}dt|u_1(t)|^{1/2}\right|, & \text{for } -\infty\le x\le x_0\\ \left|\int_{x}^{x_2}dt\,|u_1(t)|^{1/2}\right|, & \text{for } x_0\le x\le+\infty,\end{cases} \tag{56}$$

whereas for continuum states from Eqs. (24)–(25) of Ref. [5] with the turning point at $x=x_3$

$$\tfrac{2}{3}|z_2(x)|^{3/2}=\left|\int_{x_3}^{x}dt|u_2(t)|^{1/2}\right| \tag{57}$$

is obtained. There is a further useful expression, which follows from Eqs. (48) and (49) if taking partial derivatives with respect to the energies E_i,

$$\left|\frac{dx_s}{dE_i}\right|=\frac{2m}{\hbar^2}|u_1'(x_s)-u_2'(x_s)|^{-1}. \tag{58}$$

This formula makes the physical meaning of the denominator of Eq. (50) more transparent.

4. Reflection Approximations and Other Limiting Forms of Eq. (50)

We first study transitions between a *bound state potential* $V_1(x)$ and a *continuum potential* $V_2(x)$ as shown in Fig. 2. Eqs. (54), (55) yield

$$\varepsilon_1(x_a)=\varepsilon_2(x_a)=-1, \tag{59}$$

$$\varepsilon_a=+1 \tag{60}$$

and

$$\varepsilon_1(x_b)=+1,\qquad \varepsilon_2(x_b)=-1, \tag{61}$$

$$\varepsilon_b = -1. \tag{62}$$

In case of Fig. 2, Eqs. (53)–(60) imply that the argument of the Airy function in Eq. (50) is positive and large for $s = a$, i.e. x_a lies far in the classically forbidden region, $x_a < x_1 < x_3$. Since $\varepsilon_b = -1$, only the $s = b$ term in Eq. (50) can contribute significantly. Assuming that in contrast to Fig. 2 the condition

$$|z_1(x_b)| \gg |z_2(x_b)| \tag{63}$$

holds, one obtains from Eqs. (58), (53), (52), (50) and Eqs. (1)–(4) the *bound state reflection approximation*

$$M_n(E_2) \simeq \mu(x_b(E_2)) \left| \frac{dx_b(E_2)}{dE_2} \right|^{1/2} \varphi_n(x_b(E_2)), \tag{64}$$

which exactly satisfies the closure relation, see [15] Eqs. A-13, 14,

$$\int_0^\infty dE_2 \, |M_n(E_2)|^2 = \int_{-\infty}^{+\infty} dx \, \mu(x) \varphi_n^2(x). \tag{65}$$

If instead of Eq. (63)

$$|z_2(x_b)| \gg |z_1(x_b)| \tag{66}$$

holds, we obtain from Eqs. (23)–(24) of Ref. [5] in complete analogy the *continuum reflection approximation*

$$M_n(E_2) \simeq \mu(x_b(E_2)) \left(\frac{\pi}{\Phi'(E_n)} \right)^{1/2} \left| \frac{dx_b(E_2)}{dE_2} \right|^{1/2} \psi_{E_2}(x_b(E_2)). \tag{67}$$

This expression shares some similarity with the modulated continuum reflection approximation of P. M. Hunt and M. S. Child [16]. In fact Eq. (67) should be a limiting case of it.

As a final example to reflection approximations we discuss Eq. (50) for *bound–bound transitions* between a deep excimer potential $V_1(x)$ and a shallow van der Waals well $V_2(x)$ as schematically represented in Fig. 3, see also [17]. Again, only the term $s = b$ in Eq. (50) contributes since x_a lies far in the classically forbidden region of the van der Waals well. We further assume (see Fig. 3)

$$x_b \approx x_2 \tag{68}$$

and

$$|z_2(x_2)| \gg |z_1(x_2)| \approx 0. \tag{69}$$

From Eqs. (58), (48)–(55) and Eqs. (1)–(8) we obtain for the squared FC matrix element the reflection approximation

$$|M_{n_1 n_2}|^2 \simeq \frac{\pi \varphi_{n_2}^2(x_2(n_1)) \mu(x_2(n_1))}{|\Phi_1'(E_{n_1}) V_1'(x_2(n_1))|}, \tag{70}$$

where

$$V_1(x_2(n_1)) = E_{n_1}, \tag{71}$$

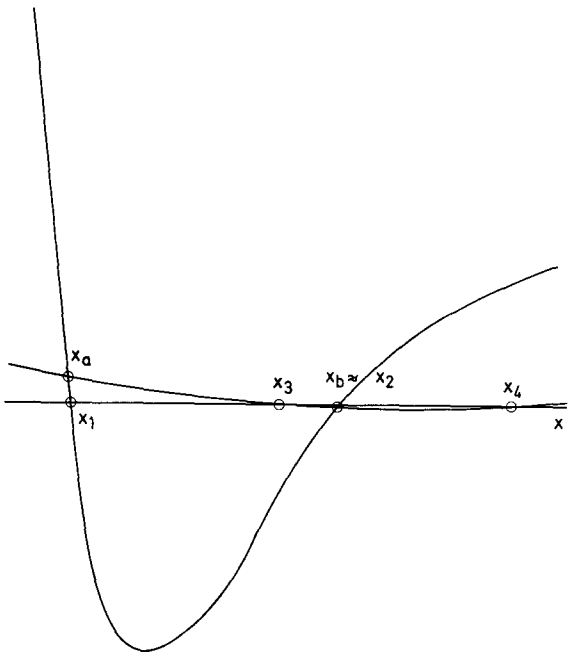

Fig. 3. Bound–bound transitions between a deep excimer potential and a shallow van der Waals well

and φ_{n_2} is the wave function of the bound vibrational state in the van der Waals well $V_2(x)$. With

$$\frac{d\Phi}{dE_1} \cdot \frac{dE_{n_1}}{dn_1} = \pi, \tag{72}$$

and the derivative of Eq. (71) with respect to n_1, Eq. (70) can be written

$$|M_{n_1 n_2}|^2 \simeq \left|\frac{dx_2(n_1)}{dn_1}\right| \varphi^2_{n_2}(x_2(n_1))\mu(x_2(n_1)) \tag{73}$$

alternatively, which shows that the semiclassical closure is satisfied. Detailed applications of Eq. (70) are defered to subsequent publications.

So far, all approximations discussed in this section involved the contribution of only one crossing point and additional simplifying assumptions have been made. In passing we note, that obviously all the one-crossing-point approximations of Refs. [1], [12–13] and [18–19] are contained in Eq. (50). Only the expression (A-25) in [15] due to K. Sando and F. H. Mies differs in its structure completely from Eq. (50). Whereas Eq. (50) uniformizes the mutual coincidence of a turning point with a crossing point and needs well separated real crossings, the Sando–Mies approach uniformizes the mutual coincidence of two crossings (real- or complex conjugate) but needs, that this occurs well separated from the turning points. We could have derived this uniformization from Eq. (27) as well by unfolding the coincidence of the two crossings within the fold catastrophe family. (The corank of Φ, Eq. (28), then is 1, Φ is 3-determined and hence its codimension

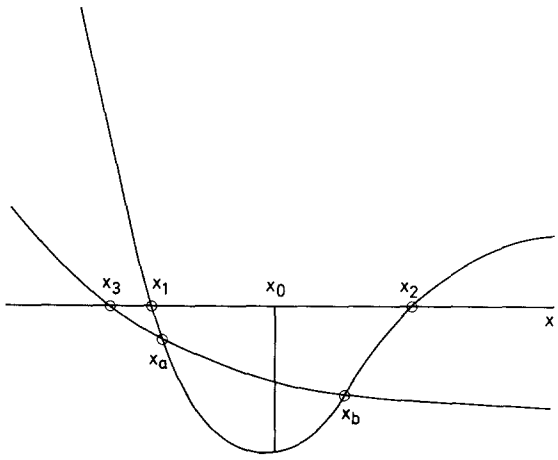

Fig. 4. Bound–continuum transitions where both crossing points x_a and x_b contribute in Eq. (50) and give rise to a highly structured continuum

is 1). As indicated in the discussion below Eq. (33), we rather refer to a forthcoming publication in which both of the above extremes are included such that even the mutual coincidence of two crossings and a turning point is permitted, which may lead to interesting "caustic effects".

In order to discuss finally at least one case for which both crossing points x_a and x_b contribute significantly to Eq. (50), we consider bound–continuum transitions with curve crossings as in Fig. 4. From Eq. (55) we obtain

$$\varepsilon_a = \varepsilon_b = -1 \tag{74}$$

and from Eq. (54)

$$\varepsilon_i(x_a) = -1, \qquad i = 1, 2, \qquad \varepsilon_1(x_b) = +1, \qquad \varepsilon_2(x_b) = -1. \tag{75}$$

Applying the asymptotic formula

$$\zeta^{1/4}\, \mathcal{A}i\,(-\zeta) \simeq \pi^{-1/2} \sin\left(\frac{\pi}{4} + \tfrac{2}{3}\zeta^{3/2}\right), \qquad \zeta \to +\infty \tag{76}$$

to Eq. (50), we finally arrive at the approximate FC matrix element

$$M_n(E_2) \simeq \left(\frac{2m}{\hbar^2 \Phi_1'(E_n)}\right)^{1/2} \left\{ \frac{(-1)^n \sin\left(\frac{\pi}{4} + \Delta_a\right)}{|u_1(x_a)|^{1/4} |V_1'(x_a) - V_2'(x_a)|^{1/2}} + \frac{\sin\left(\frac{\pi}{4} + \Delta_b\right)}{|u_1(x_b)|^{1/4} |V_1'(x_b) - V_2'(x_b)|^{1/2}} \right\}, \tag{77}$$

where, cf. Eqs. (53)–(57),

$$\Delta_s = \tfrac{2}{3}\zeta_s^{3/2}, \quad s = a, b. \tag{78}$$

Eq. (77) gives rise to interference effects which are observed e.g. in the structured $E \to B$ continuum of the I_2-molecule [10].

5. Stückelberg's Model as a Test Example

E.C.G. Stückelberg [4] derived a closed form expression for the FC integral for transitions between a harmonic ground state and the continuum of a straight line. An expression for this FC integral valid for all quantum numbers n is given in Appendix 1 of Ref. [5]. Here we discuss the matrix elements

$$M_n(\alpha, \beta) = \int_{-\infty}^{+\infty} dx\, \psi_n(\alpha + \beta x)\, \mathcal{A}i\,(-x) = \frac{1}{\beta} \int_{-\infty}^{+\infty} dx\, \psi_n(x)\, \mathcal{A}i\left(\frac{\alpha - x}{\beta}\right) \tag{79}$$

where ψ_n is given by Eq. (24). From the momentum representation of Eq. (79), obtained by use of Eq. (26),

$$M_n(\alpha, \beta) = (2\pi)^{-1/2}(-i)^n \int_{-\infty}^{+\infty} dp\, \psi_n(p)\, \mathrm{e}^{i((\beta^3/3)p^3 + \alpha p)} \tag{80}$$

and the Fourier transform

$$(2\pi)^{1/2} i^n \psi_n(\alpha) = \int_{-\infty}^{+\infty} dp\, \psi_n(p)\, \mathrm{e}^{i\alpha p} \tag{81}$$

we find the closure relation

$$\int_{-\infty}^{+\infty} d\alpha\, |M_n(\alpha, \beta)|^2 = 1 \tag{82}$$

and for $\beta = 0$ the reflection limit

$$M_n(\alpha, 0) = \psi_n(\alpha). \tag{83}$$

Eqs. (82)–(83) provide useful, but only necessary, criteria for testing approximations. The potential curves corresponding to Eq. (79) and $2m/\hbar^2 = 1$ are plotted in Fig. 5. The exact binding energies are

$$E_1 \equiv E_n = 2n + 1, \qquad n = 0, 1, 3, \ldots, \tag{84}$$

the functions $u_i(x)$, Eq. (31), are

$$u_1(x) = x^2 - E_1, \qquad u_2(x) = (\alpha - x)\beta^{-3}, \tag{85}$$

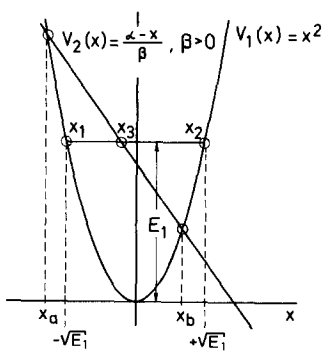

Fig. 5. The potential curves of the Stückelberg model

Table 3. The matrix elements M_n, Eq. (80), the approximation Eq. (50), $\bar{M}_n$, and the relative error $\Delta = |1 - \bar{M}_n / M_n|$ in %. The value of β is $\beta = 0.1$. The numbers in parentheses denote the power of 10 by which the value in front must be multiplied

n	α	M_n	$\bar{M}_n$	$\Delta(\%)$
	0.0	0.7511	0.7106	5.4
	0.2	0.7362	0.6984	5.1
	0.4	0.6933	0.6611	4.6
0	0.8	0.5454	0.5267	3.4
	1.6	0.2088	0.2069	0.9
	3.2	0.4488(−2)	0.4658(−2)	3.8
	5.0	0.4592(−5)	0.3084(−5)	32.8
	0.2	0.2082	0.2060	1.1
	0.4	0.3922	0.3876	1.2
1	1.0	0.6442	0.6389	0.8
	2.0	0.2875	0.2879	0.1
	3.0	0.3540(−1)	0.3592(−1)	1.5
	5.0	0.1979(−4)	0.2097(−4)	5.9
	0.0	0.4599	0.4536	1.37
	1.0	−0.4649	−0.4608	0.9
4	2.4	0.5731	0.5703	0.5
	3.0	0.3730	0.3725	0.1
	5.0	0.1259(−2)	0.1297(−2)	3.0
	7.0	0.3166(−7)	0.3504(−7)	10.6
	0.0	−0.3438	−0.3350	2.6
	0.6	0.3436	0.3343	2.7
	1.2	−0.3453	−0.3363	2.6
14	1.8	0.3526	0.3451	2.1
	2.4	−0.3621	−0.3577	1.2
	3.1	0.3798	0.3751	1.2
	3.9	−0.4083	−0.4038	1.1
	5.8	0.1398	0.1401	0.2
	0.9	−0.2646	−0.2654	0.3
	3.6	0.2591	0.2688	3.7
35	4.5	0.2975	0.2931	1.5
	5.4	0.3041	0.3048	0.2
	6.5	0.3442	0.3396	1.3
	10.0	0.6591(−3)	0.6950(−3)	5.4

and the midphase point, Eq. (7), is at $x_0 = 0$ by symmetry. Eqs. (50) and (80) have been evaluated for $\beta = 0.1$ and several values of n and α. We note that $\beta = 0.1$ as in Fig. 5 corresponds to a quite steep straight line, such that in Eq. (50) only the $s = b$ term contributes significantly. The results for M_n, Eq. (79) or even Eq. (83) and the results obtained from Eq. (50), $\bar{M}_n$, are listed in Table 3. One notes that the error of $\bar{M}_n$, with the exception of the ground state $n = 0$, is around 2%. From the experience gained by practical applications of uniform approximations like Eq. (50) such an accuracy is to be expected. But besides saving much computing time in making quantitative numerical predictions, Eq. (50) provides a quite

transparent interpretation of FC factors in terms of intermolecular potentials, a possibility not evident in the numerical exact quantum mechanical calculation.

References

1. Miller, W. H.: J. Chem. Phys. **48**, 464 (1968)
2. Langer, R. E.: Trans. Am. Math. Soc. **34**, 447 (1932); ibid. **37**, 397 (1935); ibid. **67**, 461 (1949); Bull. Am. Math. Soc. **40**, 545 (1934)
3. Mulliken, R. S.: J. Chem. Phys. **55**, 309 (1971)
4. Stückelberg, E. C. G.: Phys. Rev. **42**, 518 (1932)
5. Krüger, H.: Theoret. Chim. Acta (Berl.) **51**, 311 (1979)
6. Abramowitz, M., Stegun, I. A.: Handbook of mathematical functions. London: Dover 1965
7. Duistermaat, J. J.: Commun. Pure Appl. Math. **27**, 207 (1974)
8. Connor, J. N. L.: Mol. Phys. **31**, 33 (1976)
9. Condon, E. U.: Am. Journ. of Phys. **15**, 365 (1947)
10. Tellinghuisen, J.: Phys. Rev. Letters **34**, 1137 (1975)
11. Poston, T., Stewart, I.: Catastrophe theory and its applications. London: Pitman 1978
12. Bieniek, R. J.: Phys. Rev. **A15**, 1513 (1977)
13. Connor, J. N. L.: Uniform semiclassical evaluation of Franck–Condon factors and inelastic atom–atom scattering amplitudes, J. Chem. Phys. (in print) (1980)
14. Poston, T., Stewart, I.: Taylor expansions and catastrophes. London: Pitman 1976
15. Mies, F. H., Julienne, P. S.: IEEE J. Quantum Electron. **15**, 272 (1979)
16. Hunt, P. M., Child, M. S.: Chem. Phys. Letters **58**, 202 (1978)
17. Freeman, D. E., Yoshino, K., Tanaka, Y.: J. Chem. Phys. **71**, 1780 (1979)
18. Atabek, O., Lefebvre, R.: Chem. Phys. **23**, 51 (1977)
19. Schaefer III, H. F., Miller, W. H.: J. Chem. Phys. **55**, 4107 (1971)

Received May 2, 1980